FEBS Letters 568 (2004) 44–48 FEBS 28466

Heme environment in aldoxime dehydratase involved in carbon–nitrogen triple bond synthesis

Ken-Ichi Oinuma[a,1], Takehiro Ohta[b,1], Kazunobu Konishi[a,1], Yoshiteru Hashimoto[a], Hiroki Higashibata[a], Teizo Kitagawa[b], Michihiko Kobayashi[a,*]

[a] *Institute of Applied Biochemistry, The University of Tsukuba, 1-1-1 Tennodai, Tsukuba, Ibaraki 305-8572, Japan*
[b] *Center for Integrative Bioscience, Okazaki National Research Institutes, Myodaiji, Okazaki, Aichi 444-8585, Japan*

Received 17 March 2004; revised 27 March 2004; accepted 5 May 2004

Available online 18 May 2004

Edited by Peter Brzezinski

Abstract Resonance Raman spectra have been measured to characterize the heme environment in aldoxime dehydratase (OxdA), a novel hemoprotein, which catalyzes the dehydration of aldoxime into nitrile. The spectra showed that the ferric heme in the enzyme is six-coordinate low spin, whereas the ferrous heme is five-coordinate high spin. We assign a prominent vibration that occurs at 226 cm^{-1} in the ferrous enzyme to the Fe-proximal histidine stretching vibration. In the CO-bound form of OxdA, the correlation between the Fe–CO stretching (512 cm^{-1}) and C–O stretching (1950 cm^{-1}) frequencies also supports our assignment of proximal histidine coordination.

Keywords: Heme; Raman spectroscopy; Aldoxime; Nitrile; Dehydration; Histidine

1. Introduction

We have extensively studied the biological metabolism of toxic compounds (that have a triple bond between carbon and nitrogen) such as nitriles [R–C≡N] [1–5] and isonitriles [R–N≡C] [6,7]. The microbial degradation of nitriles proceeds through two different enzymatic pathways [8–10]: (i) nitrilase catalyzes the hydrolysis of nitriles into acids [R–C(=O)–OH] and ammonia [11–13]; and (ii) nitrile hydratase (NHase) catalyzes the hydration of nitriles to amides [R–C(=O)–NH_2] [14–17], which are subsequently hydrolyzed to acids and ammonia by amidase [18–20]. These enzymes have received much attention in applied fields [2,8,21] as well as academic ones [13,22–26]. One of the fruits of our application-oriented nitrile studies is the current industrial production of acrylamide and nicotinamide using NHase of an actinomycete, *Rhodococcus rhodochrous* J1 [1,9]. On the other hand, NHase of *Pseudomonas chlororaphis* B23 [27], which was previously used as a catalyst for acrylamide manufacture [9,21,28], is now used for the production of 5-cyanovaleramide, a herbicide intermediate, at the industrial level [29]. We have already cloned the NHase gene from this strain and discovered the existence of a gene cluster including the NHase and amidase genes [30].

Very recently, we discovered a gene (*oxdA*) encoding a novel nitrile-synthesizing enzyme (aldoxime dehydratase) upstream of the NHase and amidase genes in *P. chlororaphis* B23 [31]. The amino acid sequence of OxdA shows similarity (32% identity) with that of *Bacillus* phenylacetaldoxime dehydratase [32]. OxdA [31] and phenylacetaldoxime dehydratase are novel heme proteins including protoheme IX as the prosthetic group. These enzymes catalyze a unique and intriguing reaction: formation of a carbon–nitrogen triple bond and dehydration of a substrate [R–CH=N–OH] in spite of the presence of water in the reaction mixture. This reaction is not only academically interesting but also expected to be applicable to the practical production of nitriles because it is performed under mild conditions in contrast with chemical dehydration of aldoximes under harsh conditions [33]. It was previously reported that rat liver microsomal cytochromes P450 and P450 3A4 [34] (the major P450 isozyme in human liver), whose sequence exhibits no similarity to that of the aldoxime dehydratase family (comprising OxdA and phenylacetaldoxime dehydratase), also catalyze the dehydration of aldoxime; but their catalytic activities are not so high. It is noteworthy that these aldoxime dehydration reactions would involve the direct approach of the substrate to the heme iron in the microsomal P450s [34] or OxdA [31], in contrast with various other reactions (e.g., monooxygenation) of general hemoproteins. Although the P450 enzymes are known to have cysteine as the proximal ligand [34], the heme environmental structure (including a proximal ligand) of the aldoxime dehydratase family remains unknown. In the present study, for the first time, we characterized the heme environment in OxdA using resonance Raman spectroscopy.

2. Materials and methods

2.1. Expression and purification of recombinant OxdA

OxdA was overexpressed as described previously [31] with a few improvements. *Escherichia coli* BL21-CodonPlus(DE3)-RIL was

* Corresponding author. Fax: +81-29-853-4605 (Institute).

[1] These authors contributed equally to the results of this work.

Abbreviations: NHase, nitrile hydratase; OxdA(CO), the CO-bound form of OxdA; HRP, horseradish peroxidase; Hb, hemoglobin; *Sw* Mb, sperm whale myoglobin; *Mt* Hb, *Mycobacterium tuberculosis* hemoglobin; *Pc* Hb, *Paramecium caudatum* hemoglobin; *Rm* FixL*, soluble truncated domain of *Rhizobium meliloti* FixL; HO, heme-bound heme oxygenase; sGC, soluble guanylate cyclase

0014-5793/$22.00 © 2004 Published by Elsevier B.V. on behalf of the Federation of European Biochemical Societies.
doi:10.1016/j.febslet.2004.05.008

transformed with pET-*oxdA*. The transformed cells were incubated with reciprocal shaking at 37 °C in 800 ml of 2× YT medium containing 50 μg/ml kanamycin and 34 μg/ml chloramphenicol. After overnight cultivation, the entire culture was inoculated into 80 l of the same medium, followed by incubation with shaking at 37 °C for 2 h. IPTG was then added to a final concentration of 0.1 mM to induce the T7 promoter and further cultivation was carried out at 20 °C for 30 h.

OxdA was purified from the *E. coli* transformant expressing OxdA by a modification of the previously reported procedure [31]. All steps were performed at 0–4 °C. Potassium phosphate buffer (pH 7.0) without 2-mercaptoethanol was used throughout the purification. Centrifugation was carried out for 30 min at $15\,000 \times g$.

The cells were harvested by centrifugation, washed twice with 100 mM buffer, and then disrupted by sonication (Insonator Model 201M; Kubota, Tokyo, Japan) to prepare a cell-free extract. Cell debris was removed by centrifugation. The resulting supernatant was fractionated with ammonium sulfate (35–60% saturation), followed by dialysis against 10 mM buffer. The dialyzed solution was applied to a DEAE–Sephacel column (5 × 25 cm) (Amersham Biosciences, Piscataway, NJ) equilibrated with 10 mM buffer. Protein was eluted from the column with 2.0 liters of 10 mM buffer, the concentration of KCl being increased linearly from 0.1 to 0.5 M. This operation on the DEAE–Sephacel column was separately performed twice because of the capacity limitation. The active fractions were collected and then ammonium sulfate was added to give 20% saturation. The enzyme solution was placed on a TSK gel Butyl-Toyopearl 650 M column (5 × 25 cm) (Tosoh Co., Tokyo, Japan) equilibrated with 10 mM buffer 20% saturated with ammonium sulfate. The enzyme was eluted by lowering the concentration of ammonium sulfate (20–0%) in 2.0 l of the same buffer. This operation on the Butyl-Toyopearl column was separately performed twice because of the capacity limitation. The active fractions were combined and then precipitated with ammonium sulfate at 70% saturation. The precipitate was collected by centrifugation, dissolved in 0.1 M buffer, and then dialyzed against three changes of 5 l of 1 mM buffer (pH 6.8). After centrifugation, the enzyme solution was loaded on a Cellulofine HAp column (5 × 25 cm) (Seikagaku Kogyo Co., Tokyo, Japan) equilibrated with 1 mM buffer (pH 6.8). The column was eluted with a linear gradient, 1–100 mM, of the buffer (pH 6.8). The resultant solution was dialyzed against 10 mM buffer and then centrifuged. The active fractions were collected and then ammonium sulfate was added to give 70% saturation. After centrifugation of the suspension, the precipitate was dissolved in 0.1 M buffer and then dialyzed against 10 mM buffer. The homogeneity of the purified protein was confirmed by SDS–PAGE.

2.2. Analytical methods

The heme content was estimated by the pyridine ferrohemochrome method as previously reported [31]. Protein concentrations were determined with a Nakalai Tesque Co., Inc. (Kyoto, Japan) protein assay kit, with bovine serum albumin as the standard.

The reduction of OxdA was carried out by adding a few grains of sodium dithionite to the isolated OxdA. CO gas was introduced into the OxdA solution by means of a gastight syringe.

2.3. Spectral measurements

Resonance Raman spectra were obtained with laser excitation at 413.1 nm with a Kr^+ laser (Spectra Physics, model 2060) or at 430 nm with a diode laser (Hitachi Metal, 58-BTLR010). The excitation light was focused into the cell, and the laser power was 3 mW at the cell for the isolated and reduced forms of OxdA, but 0.005–0.5 mW for the CO-bound OxdA. The sample solutions for the Raman measurements were sealed in quartz cells, which were rotated at 1500 rpm at room temperature. Typically, 50 μl sample aliquots of 30 μM protein in 100 mM potassium phosphate buffer, pH 7.0, were put into the cell. The scattered light was dispersed with a single polychromator (Ritsu, DG-1000) equipped with a liquid nitrogen-cooled charge-coupled device (CCD) camera. The spectral slit width was 6 cm^{-1}. Raman shifts were calibrated using indene, CCl_4, and an aqueous solution of potassium ferrocyanide as frequency standards, providing an accuracy of ±1 cm^{-1} for intense isolated lines.

3. Results and discussion

3.1. Establishment of a thorough purification procedure for OxdA

We previously reported the use of 2-mercaptoethanol in the buffer for the purification of OxdA [31]. However, we found here that 2-mercaptoethanol was not required for the stability or activity of the enzyme, rather it led to a decrease in the heme content. Although the previously purified enzyme contained only 0.69 mol of heme/mol of subunit, we have succeeded in obtaining purified OxdA containing 1.06 mol of heme/mol of subunit using the novel purification scheme described in Section 2. Using the newly purified OxdA, here, we succeeded in obtaining fine spectroscopic results for the first time.

3.2. High-frequency resonance Raman spectroscopy

It has been established that resonance Raman spectra in the high-frequency region contain a few marker bands sensitive to the oxidation state (ν_4), and spin and coordination states (ν_2 and ν_3) of the heme iron in so far known hemoproteins [35]. The resonance Raman spectra in the high-frequency region (1300–1700 cm^{-1}) of the purified OxdA, a ferrous form (the active state), and its CO adduct [OxdA(CO)] are shown in Fig. 1. The purified OxdA gave ν_2, ν_3 and ν_4 bands at 1574, 1502, and 1376 cm^{-1}, respectively. These frequencies suggest that the purified OxdA contains a six-coordinate low-spin ferric heme. The ferrous form, which is the active state of OxdA, gave ν_2, ν_3 and ν_4 bands at 1557, 1471, and 1358 cm^{-1}, respectively, at typical frequencies of the five-coordinate high-spin ferrous hemes. This indicates that ferrous OxdA has a free distal heme pocket; similar to those of horseradish peroxidase (HRP) [36] and hemoglobin (Hb) [37], which enables aldoximes to easily gain access to the heme iron. OxdA(CO) gave ν_2,

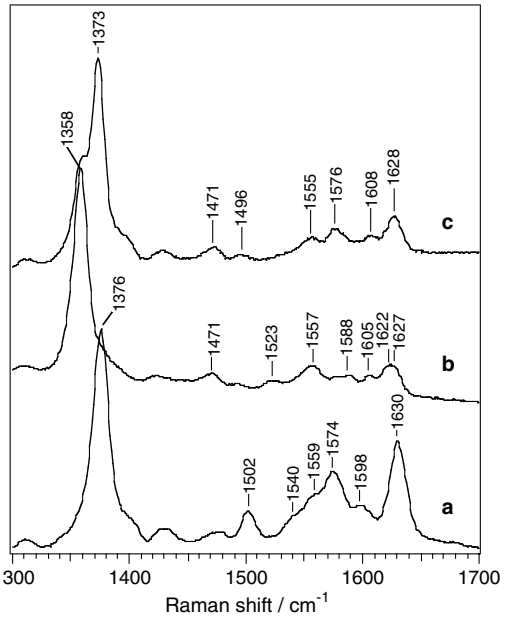

Fig. 1. High-frequency regions of resonance Raman spectra of the purified OxdA (a), the ferrous form (b), and the CO adduct (c). The spectra were acquired as described in Section 2, using 413.1 nm excitation for the purified OxdA and OxdA(CO), and 430 nm excitation for ferrous OxdA (3 mW for the purified OxdA and ferrous OxdA, and 0.005 mW for the CO adduct).

ν_3 and ν_4 bands at 1576, 1496, and 1373 cm^{-1}, respectively, at frequencies characteristic of a six-coordinate low-spin CO-ligated heme. However, OxdA(CO) exhibited extreme photolability, which prevented us from obtaining a Raman spectrum for the pure CO adduct. For OxdA(CO), therefore, we had to use very low laser power: 5–10 μW for both the high- and low-frequency regions. It is worth noting that its photosensitivity is distinct from that for HRP and Hb, indicating the peculiarity of the OxdA heme pocket.

3.3. Fe–His stretching mode

The low-frequency resonance Raman spectra of ferrous OxdA and OxdA(CO) are shown in Fig. 2. An intense band at 226 cm^{-1}, which was undetectable with the CO adduct (a), was observed for ferrous OxdA (d) and the photoproduct (b, c) of the CO adduct. For the other previously reported hemoproteins, the Fe–N_{His} stretching band is generally observable in the region from 200 to 230 cm^{-1} for the five-coordinated ferrous hemes containing an imidazole axial ligand but not for six-coordinated ferrous hemes [38]. We therefore assigned the 226 cm^{-1} band to Fe–His stretching, ν_{Fe-His} of ferrous OxdA. This band appears around 220 cm^{-1} when the coordinated imidazole is not hydrogen bonded but below it when some strain from protein is present. In contrast, the band is shifted to a higher frequency when the imidazole is hydrogen bonded. The observed frequency for OxdA means the presence of a moderately strong hydrogen bond.

3.4. Fe–C–O modes in the CO-bound OxdA

The CO-isotope dependence of resonance Raman spectra of OxdA(CO) is shown in Figs. 3 and 4. Isotope shifts of 32 and 20 cm^{-1} were observed for the bands at 512 and 579 cm^{-1}, respectively, upon substitution of $^{13}C^{18}O$ for $^{12}C^{16}O$ (Fig. 3). For the band at 1950 cm^{-1}, isotope shifts of 50 and 52 cm^{-1} were observed upon substitution of $^{13}C^{16}O$ and $^{12}C^{18}O$, respectively, for $^{12}C^{16}O$ (Fig. 4). Based on the frequencies of these bands and the sizes of the isotope shifts, we assigned the 512, 579, and 1950 cm^{-1} bands to the Fe–CO stretching (ν_{Fe-CO}), Fe–C–O bending (δ_{Fe-C-O}), and C–O stretching (ν_{C-O}) modes, respectively.

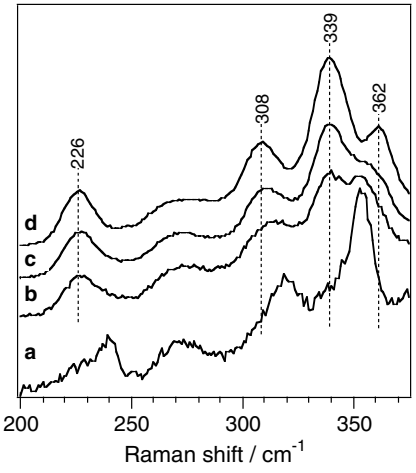

Fig. 2. Low-frequency regions of resonance Raman spectra of ferrous OxdA (d) and its CO adduct (a)–(c). The spectra were acquired as described in Section 2, using 430 nm excitation. Laser power: (a) 0.01 mW; (b) 0.1 mW; (c) 0.5 mW; (d) 3 mW.

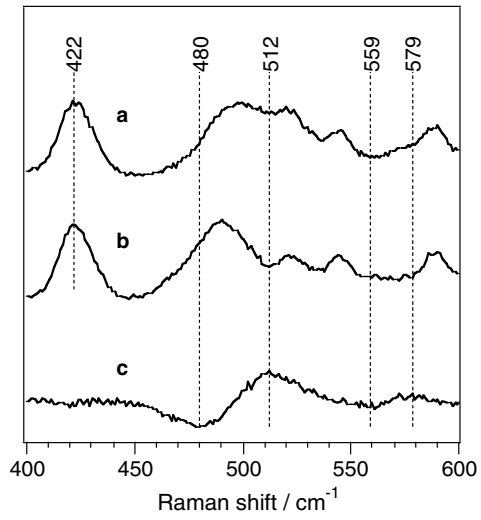

Fig. 3. The resonance Raman spectra in the Fe–CO stretching and Fe–C–O bending regions of OxdA($^{12}C^{16}O$) and OxdA($^{13}C^{18}O$), and their difference spectra: (a) OxdA($^{12}C^{16}O$); (b) OxdA($^{13}C^{18}O$); (c) (a)–(b) difference spectrum.

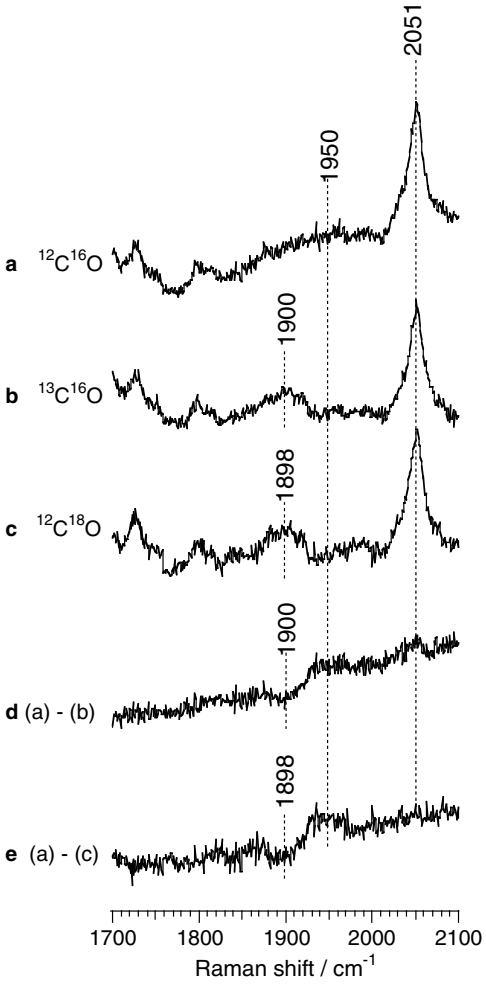

Fig. 4. The resonance Raman spectra in the C–O stretching region of OxdA($^{12}C^{16}O$), OxdA($^{13}C^{16}O$), and OxdA($^{12}C^{18}O$), and their difference spectra: (a) OxdA($^{12}C^{16}O$); (b) OxdA($^{13}C^{16}O$); (c) OxdA($^{12}C^{18}O$); (d) (a)–(b) difference spectrum; (e) (a)–(c) difference spectrum.

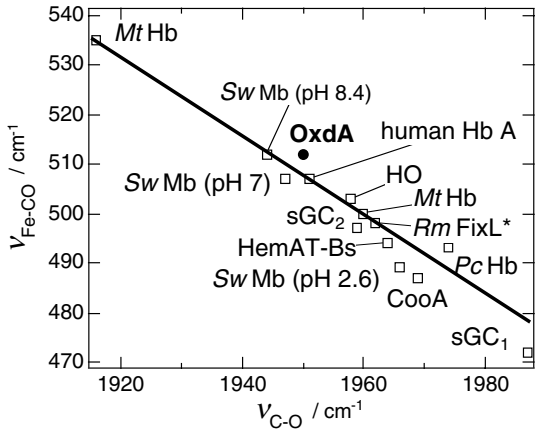

Fig. 5. A plot of ν_{Fe-CO} frequencies against ν_{C-O} frequencies observed for CO-bound hemoproteins. The Raman data for *Mycobacterium tuberculosis* hemoglobin (*Mt* Hb), *Paramecium caudatum* hemoglobin (*Pc* Hb), HemAT-Bs, heme-bound heme oxygenase (HO), soluble truncated domain of *Rhizobium meliloti* FixL (*Rm* FixL*), soluble guanylate cyclases (sGC_1, sGC_2), CooA, human Hb A and sperm whale myoglobin (*Sw* Mb) (pH 2.6, 7.0 and 8.4) are cited from [41] and references therein.

There is a well-established correlation between the frequencies of the Fe–CO stretching and C–O stretching modes spanning many different heme proteins and model complexes [39,40]. The correlation depends on the nature of the proximal ligand; the CO-bound hemes with an imidazole/histidine as the *trans* ligand exhibit a correlation line different from those with a thiolate or imidazolate. The ν_{Fe-CO} and ν_{C-O} bands of OxdA(CO), which were detected at 512 and 1950 cm^{-1}, respectively, fell on the imidazole/histidine correlation line, as illustrated in Fig. 5. This finding confirms our assignment of neutral imidazole coordination. An additional indication of the distal heme pocket is also given by the Fe–CO and C–O stretching modes.

There are two well known factors governing the Fe–CO stretching frequency in CO-bound heme species. The first is the nature of the axial ligand *trans* to the bound CO. If the ligand is a weak electron donor or absent, relatively high frequencies are found for Fe–CO stretching because the competition for the metal σ orbital is not severe [42]. The second factor is the polarity of the environment around the bound CO [43–45]. Positive charges near the oxygen atom of CO enhance π-back bonding from Fe^{2+} to CO and, as a result, decrease ν_{C-O} and increase ν_{Fe-CO}. On the other hand, negative charges inhibit the π-back bonding, and thereby increase ν_{C-O} and decrease ν_{Fe-CO}. OxdA exhibited a relatively high ν_{Fe-His} (226 cm^{-1}) compared with other hemoproteins containing an imidazole axial ligand, and therefore, a weak Fe–CO bond was expected considering the above mentioned first factor governing ν_{Fe-CO} frequency. However, the observed ν_{Fe-CO} of OxdA (512 cm^{-1}) is higher than those of many other hemoproteins which have weaker Fe–His bond, including myoglobin ($\nu_{Fe-CO} = 507$ cm^{-1}) [43]. Together with the second factor, these findings for OxdA indicate that there are positively charged or proton donating residues in the distal pocket. On the other hand, we should also notice that there are rare cases where a structural change in the proximal environment occurs upon CO binding, affecting the ν_{Fe-CO} frequency. The Raman data on *Alcaligenes xylosoxidans* cytochrome c' show that the proximal histidine of the cytochrome c' is deprotonated in the ferrous state, but protonated in the CO adduct, suggesting that the structure in the proximity of heme changes upon CO binding [46]. In the case of OxdA, the hydrogen bonding between the proximal histidine and the counterpart could be broken upon CO binding, leading to a weakening of the Fe–His bond and the concomitant increase of the ν_{Fe-CO} frequency.

In the present study, we have characterized the heme environmental structure of OxdA. The axial ligand type of OxdA is completely different from that of the P450 enzymes. In order to clarify the details of the function and structure of OxdA, site-directed mutagenesis, further spectroscopic analysis, and the X ray crystallography of OxdA are currently in progress.

Acknowledgements: We thank Dr. Naoki Takaya (The University of Tsukuba) for the valuable discussions. This work was supported in part by the 21st Century COE Program of the Ministry of Education, Culture, Sports, Science, and Technology (MEXT), by a Grant-in-Aid for Scientific Research from the Ministry of Education, Science and Culture of Japan, by the Industrial Technology Research Grant Program in '02 of the New Energy and Industrial Technology Development Organization (NEDO) of Japan, by the National Project on Protein Structural and Functional Analyses, and by a Research Grant (A) of the University Research Projects.

References

[1] Kobayashi, M. and Shimizu, S. (1998) Nat. Biotechnol. 16, 733–736.
[2] Kobayashi, M. and Shimizu, S. (2000) Curr. Opin. Chem. Biol. 4, 95–102.
[3] Komeda, H., Kobayashi, M. and Shimizu, S. (1996) J. Biol. Chem. 271, 15796–15802.
[4] Komeda, H., Kobayashi, M. and Shimizu, S. (1996) Proc. Natl. Acad. Sci. USA 93, 4267–4272.
[5] Kobayashi, M., Komeda, H., Yanaka, N., Nagasawa, T. and Yamada, H. (1992) J. Biol. Chem. 267, 20746–20751.
[6] Goda, M., Hashimoto, Y., Shimizu, S. and Kobayashi, M. (2001) J. Biol. Chem. 276, 23480–23485.
[7] Goda, M., Hashimoto, Y., Takase, M., Herai, S., Iwahara, Y., Higashibata, H. and Kobayashi, M. (2002) J. Biol. Chem. 277, 45860–45865.
[8] Kobayashi, M., Nagasawa, T. and Yamada, H. (1992) Trends Biotechnol. 10, 402–408.
[9] Yamada, H. and Kobayashi, M. (1996) Biosci. Biotechnol. Biochem. 60, 1391–1400.
[10] Kobayashi, M. and Shimizu, S. (1994) FEMS Microbiol. Lett. 120, 217–224.
[11] Kobayashi, M., Yanaka, N., Nagasawa, T. and Yamada, H. (1992) Biochemistry 31, 9000–9007.
[12] Komeda, H., Hori, Y., Kobayashi, M. and Shimizu, S. (1996) Proc. Natl. Acad. Sci. USA 93, 10572–10577.
[13] Kobayashi, M., Izui, H., Nagasawa, T. and Yamada, H. (1993) Proc. Natl. Acad. Sci. USA 90, 247–251.
[14] Kobayashi, M., Suzuki, T., Fujita, T., Masuda, M. and Shimizu, S. (1995) Proc. Natl. Acad. Sci. USA 92, 714–718.
[15] Kobayashi, M. and Shimizu, S. (1999) Eur. J. Biochem. 261, 1–9.
[16] Asano, Y., Tani, Y. and Yamada, H. (1980) Agric. Biol. Chem. 44, 2251–2252.
[17] Popescu, V.C., Munck, E., Fox, B.G., Sanakis, Y., Cummings, J.G., Turner Jr., I.M. and Nelson, M.J. (2001) Biochemistry 40, 7984–7991.
[18] Kobayashi, M., Fujiwara, Y., Goda, M., Komeda, H. and Shimizu, S. (1997) Proc. Natl. Acad. Sci. USA 94, 11986–11991.
[19] Kobayashi, M., Goda, M. and Shimizu, S. (1998) FEBS Lett. 439, 325–328.
[20] Kobayashi, M., Komeda, H., Nagasawa, T., Nishiyama, M., Horinouchi, S., Beppu, T., Yamada, H. and Shimizu, S. (1993) Eur. J. Biochem. 217, 327–336.
[21] Yamada, H., Shimizu, S. and Kobayashi, M. (2001) Chem. Records 1, 152–161.

[22] Normanly, J., Grisafi, P., Fink, G.R. and Bartel, B. (1997) Plant Cell 10, 1781–1790.
[23] Bartling, D., Seedorf, M., Schmidt, R.C. and Weiler, E.W. (1994) Proc. Natl. Acad. Sci. USA 91, 6021–6025.
[24] Pekarsky, Y., Campiglio, M., Siprashvili, Z., Druck, T., Sedkov, Y., Tillib, S., Draganescu, A., Wermuth, P., Rothman, J.H., Huebner, K., Buchberg, A.M., Mazo, A., Brenner, C. and Croce, C.M. (1998) Proc. Natl. Acad. Sci. USA 95, 8744–8749.
[25] Endo, I., Odaka, M. and Yohda, M. (1999) Trends Biotechnol. 17, 244–248.
[26] Cravatt, B.F., Giang, D.K., Mayfield, S.P., Boger, D.L., Lerner, R.A. and Gilula, N.B. (1996) Nature 384, 83–87.
[27] Nagasawa, T., Nanba, H., Ryuno, K., Takeuchi, K. and Yamada, H. (1987) Eur. J. Biochem. 162, 691–698.
[28] Nagasawa, T., Ryuno, K. and Yamada, H. (1989) Experientia 45, 1066–1070.
[29] Hann, E.C., Eisenberg, A., Fager, S.K., Perkins, N.E., Gallagher, F.G., Cooper, S.M., Gavagan, J.E., Stieglitz, B., Hennessey, S.M. and DiCosimo, R. (1999) Bioorg. Med. Chem. 7, 2239–2245.
[30] Nishiyama, M., Horinouchi, S., Kobayashi, M., Nagasawa, T., Yamada, H. and Beppu, T. (1991) J. Bacteriol. 173, 2465–2472.
[31] Oinuma, K.-I., Hashimoto, Y., Konishi, K., Goda, M., Noguchi, T., Higashibata, H. and Kobayashi, M. (2003) J. Biol. Chem. 278, 29600–29608.
[32] Kato, Y., Nakamura, K., Sakiyama, H., Mayhew, S.G. and Asano, Y. (2000) Biochemistry 39, 800–809.
[33] Xie, S.X., Kato, Y. and Asano, Y. (2001) Biosci. Biotechnol. Biochem. 65, 2666–2672.
[34] Boucher, J.L., Delaforge, M. and Mansuy, D. (1994) Biochemistry 33, 7811–7818.
[35] Spiro, T.G. and Li, X.-Y. (1988) in: Biological Applications of Raman Spectroscopy (Spiro, T.G., Ed.), vol. III, pp. 1–37, Wiley, New York.
[36] Rakshit, G. and Spiro, T.G. (1974) Biochemistry 13, 5317–5323.
[37] Spiro, T.G. and Strekas, T.C. (1974) J. Am. Chem. Soc. 96, 338–345.
[38] Kitagawa, T. (1988) in: Biological Applications of Raman Spectroscopy (Spiro, T.G., Ed.), vol. III, pp. 97–131, Wiley, New York.
[39] Yu, N.-T. and Kerr, E.A. (1988) in: Biological Applications of Raman Spectroscopy (Spiro, T.G., Ed.), vol. III, pp. 39–95, Wiley, New York.
[40] Uno, T., Nishimura, Y., Tsuboi, M., Makino, R., Iizuka, T. and Ishimura, Y. (1987) J. Biol. Chem. 262, 4549–4556.
[41] Aono, S., Kato, T., Matsuki, M., Nakajima, H., Ohta, T., Uchida, T. and Kitagawa, T. (2002) J. Biol. Chem. 277, 13528–13538.
[42] Kerr, E.A., Mackin, H.C. and Yu, N.-T. (1983) Biochemistry 22, 4373–4379.
[43] Ray, G.B., Li, X.-Y., Ibers, J.A., Sessler, J.L. and Spiro, T.G. (1994) J. Am. Chem. Soc. 116, 162–176.
[44] Kushkuley, B. and Stavrov, S.S. (1996) Biophys. J. 70, 1214–1229.
[45] Phillips Jr., G.N., Teodoro, M.L., Li, T., Smith, B. and Olson, J.S. (1999) J. Phys. Chem. B 103, 8817–8829.
[46] Andrew, C.R., Green, E.L., Lawson, D.M. and Eady, R.R. (2001) Biochemistry 40, 4115–4122.